

Chapter VII: Cold plasma reactors

•“Thin film processes”, J.L. Vossem and W. Kern editors, Academic Press (1978). ISBN:0-12-728250-5.

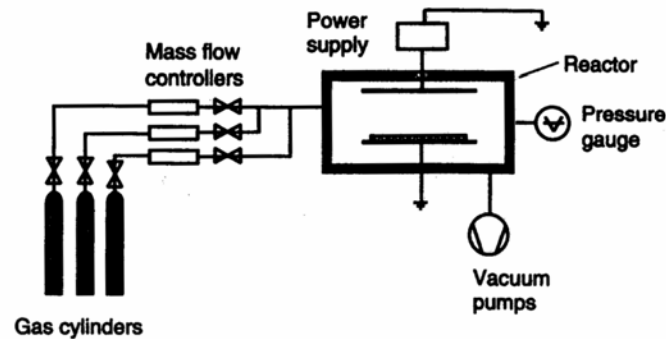
•“Industrial Plasma Engineering”, J.R. Roth, Institute of Physics Publishing, (1995). ISBN: 0-7503-0317-4

•“Principle of plasma discharges and materials processing”, M. Lieberman and A.J. Lichtenberg, (2005), ISBN: 0-471-72001-1

Content

1. Plasma systems
2. Gaz liquid suppliers
 - 2.1 MFC
 - 2.2 LFC
3. Reactors
 - 3.1 Diode
 - 3.2 Magnetrons system
 - 3.2.1 Balanced
 - 3.2.2 Unbalanced
 - 3.2.3 Reactive sputtering
 - 3.2.4 Pulsed sputtering
 - 3.2.5 Special magnetron
 - 3.3 RF
 - 3.3.1 Electrode less discharge
 - 3.3.2 Electrode discharge
 - 3.4 μ W
 - 3.4.1 Non ECR
 - 3.4.2 ECR

1. Plasma systems



General outline of a system for cold plasma processing.

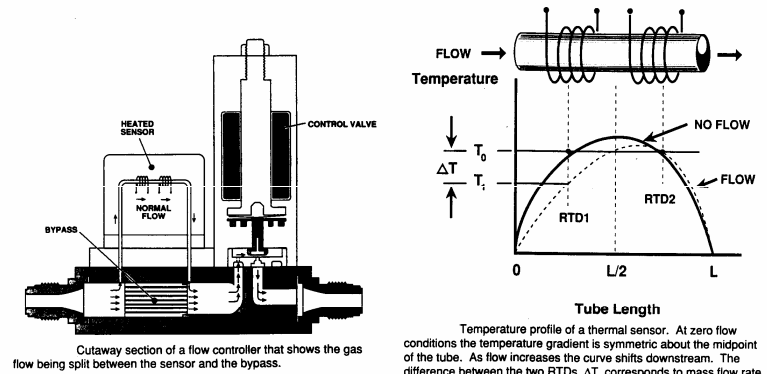
Several subsystems including:

- Gas supply: gas in high pressure cylinder or liquid/solids with high vapour pressures.
- Mass flow controllers
- Vacuum pumping and measurement system:
- Operating pressures: $1 \times 10^{-4} \rightarrow \sim 10$ torr
- Measurement systems: capacitance gauge
- Plasma reactor
- Power supplies: twofold: excite the plasma, control the bias.
- Safety devices: Corrosive, highly toxic, flammable or explosive gas
- Flow limiters, Flashback attestors, Scrubbers,

2. Gas/liquid suppliers

2.1 Gas flow controllers

Control carrier gases, reactive and purging gases.



Cutaway section of a flow controller that shows the gas flow being split between the sensor and the bypass.

Temperature profile of a thermal sensor. At zero flow conditions the temperature gradient is symmetric about the midpoint of the tube. As flow increases the curve shifts downstream. The difference between the two RTDs, ΔT , corresponds to mass flow rate.

MF are calculated by measuring the change in gas temperature as it passes through the heater. Typically, MFC's are calibrated at the manufacturer's facility for nitrogen gas. For other gases, it is necessary to use a gas correction factor.

2. Gas/liquid suppliers

GAS CORRECTION FACTOR CHART (CONT.)

GAS	SYMBOL	SPECIFIC HEAT, Cp cal/g°C	DENSITY g/l @ 0°C	CORRECTION FACTOR
Freon - 1132A	C ₂ H ₂ F ₂	.224	2.857	.43
Helium	He	1.241	.1786	1.454
Hexafluoroethane (Freon - 116)	F ₃ CCF ₃	.1843	6.157	.24
Hydrogen	H ₂	3.419	.0899	1.01
Hydrogen Bromide	HBr	.0861	3.610	1.00
Hydrogen Chloride	HCl	.1912	1.627	1.00
Hydrogen Fluoride	HF	.3479	.893	1.00
Isobutylene	C ₄ H ₈	.3701	2.503	.29
Krypton	Kr	.0593	3.739	1.543
Methane	CH ₄	.5328	.715	.72
Methyl Fluoride	CH ₃ F	.3221	1.518	.58
Molybdenum Hexafluoride	MoF ₆	.1373	9.366	.21
Neon	Ne	.246	.900	1.46
Nitric Oxide	NO	.2328	1.339	.99
Nitrogen	N ₂	.2485	1.250	1.00
Nitrogen Dioxide	NO ₂	.1933	2.052	.74
Nitrogen Trifluoride	NF ₃	.1797	3.168	.48
Nitrous Oxide	N ₂ O	.2088	1.964	.71
Octafluorocyclobutane (Freon - C318)	C ₄ F ₈	.185	8.937	.17
Oxygen	O ₂	.2193	1.427	1.00
Pentane	C ₅ H ₁₂	.398	3.219	.21
Perfluoropropane	C ₃ F ₈	.194	8.388	.17
Phosgene	COCl ₂	.1394	4.418	.44
Phosphine	PH ₃	.2374	1.517	.76
Propane	C ₃ H ₈	.3885	1.967	.36
Propylene	C ₃ H ₆	.3541	1.877	.41
Silane	SiH ₄	.3189	1.433	.60
Silicon Tetrachloride	SiCl ₄	.1270	7.580	.28
Silicon Tetrafluoride	SiF ₄	.1691	4.643	.35
Sulfur Dioxide	SO ₂	.1488	2.858	.69
Sulfur Hexafluoride	SF ₆	.1592	6.516	.26
Trichlorofluoromethane (Freon - 111)	CCl ₃ F	.1357	6.129	.33
Trichlorosilane	SiHCl ₃	.1380	6.043	.33
1, 1, 2 - Trichloro - 1, 2, 2 Tetrafluoroethane (Freon - 113)	CCl ₂ FCClF ₂	.161	8.360	.20
Tungsten Hexafluoride	WF ₆	.0810	13.28	.25
Xenon	Xe	.0378	5.858	1.32

Novembre 2008

VII.5 Plasma, S. Lucas

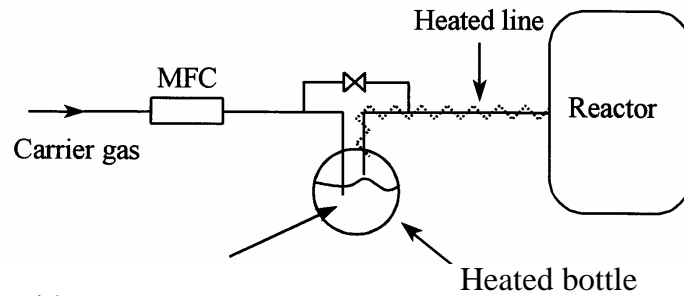
2. Gas/liquid suppliers

GAS CORRECTION FACTOR CHART

GAS	SYMBOL	SPECIFIC HEAT, Cp cal/g°C	DENSITY g/l @ 0°C	CORRECTION FACTOR
Air	---	.240	1.293	1.00
Ammonia	NH ₃	.492	.760	.73
Argon	Ar	.1244	1.782	1.45
Arsine	AsH ₃	.1167	3.478	.67
Boron Trichloride	BCl ₃	.1279	5.227	.41
Bromine	Br ₂	.0539	7.130	.81
Carbon Dioxide	CO ₂	.2016	1.964	.74
Carbon Monoxide	CO	.2488	1.250	1.00
Carbon Tetrachloride	CCl ₄	.1655	6.86	.31
Carbon Tetrafluoride (Freon - 14)	CF ₄	.1654	3.926	.42
Chlorine	Cl ₂	.1144	3.163	.86
Chlorodifluoromethane (Freon - 22)	CHClF ₂	.1544	3.858	.46
Chloropentafluoroethane (Freon - 115)	C ₂ ClF ₅	.164	6.892	.24
Chlorotrifluoromethane (Freon - 13)	CClF ₃	.153	4.660	.38
Cyanogen	C ₂ N ₂	.2613	2.322	.61
Deuterium	D ₂	1.722	1.799	1.00
Diborane	B ₂ H ₆	.508	1.235	.44
Dibromodifluoromethane	CBBr ₂ F ₂	.15	9.362	.19
Dichlorodifluoromethane (Freon - 12)	CCl ₂ F ₂	.1432	5.395	.35
Dichlorofluoromethane (Freon - 21)	CHCl ₂ F	.140	4.592	.42
Dichloromethylsilane	(CH ₃) ₂ SiCl ₂	.1882	5.758	.25
Dichlorosilane	SiH ₂ Cl ₂	.150	4.506	.40
1, 2 - Dichlorotetrafluoroethane (Freon - 114)	C ₂ Cl ₂ F ₄	.160	7.626	.22
1, 1 - Difluoroethylene (Freon - 1132A)	C ₂ H ₂ F ₂	.224	2.857	.43
2, 2 - Dimethylpropane	C ₄ H ₁₀	.3914	3.219	.22
Ethane	C ₂ H ₆	.4097	1.342	.50
Fluorine	F ₂	.1873	1.695	.98
Fluoroform (Freon - 23)	CHF ₃	.176	3.127	.50
Freon - 11	CCl ₃ F	.1357	6.129	.33
Freon - 12	CCl ₂ F ₂	.1432	5.395	.35
Freon - 13	CClF ₃	.153	4.660	.38
Freon - 13 B.	CBrF ₃	.1113	6.644	.37
Freon - 14	CF ₄	.1654	3.926	.42
Freon - 21	CHCl ₂ F	.140	4.592	.42
Freon - 22	CHClF ₂	.1544	3.858	.46
Freon - 23	CHF ₃	.176	3.127	.50
Freon - 113	CCl ₂ FCClF ₂	.161	8.360	.20
Freon - 114	C ₂ Cl ₂ F ₄	.160	7.626	.22
Freon - 115	C ₂ ClF ₅	.164	6.892	.24
Freon - 116	F ₃ CCF ₃	.1843	6.157	.24
Freon - C318	C ₄ F ₈	.185	8.397	.17

2. Gas/liquid suppliers

2.2 Liquid flow controllers



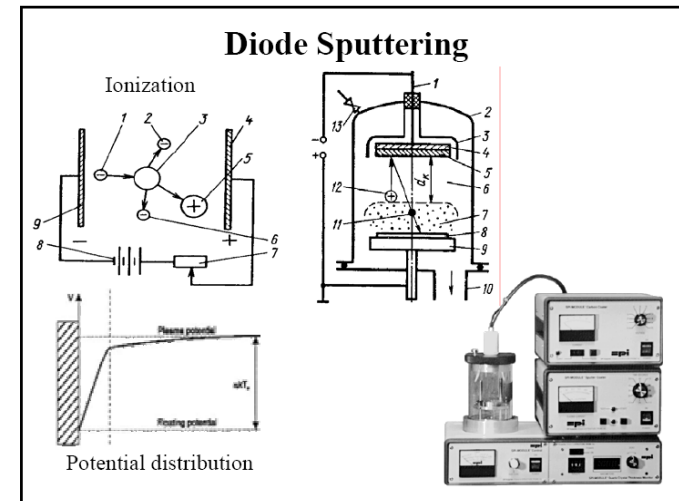
Liquid reactant:

TEOS ($\text{Si}(\text{OC}_2\text{H}_5)_4$)

TMA ($(\text{CH}_3)_3\text{Al}$)

3. Reactors and deposition

3.1 DC-DIODE system



Characteristics:

- Electrode spacing: 5 -10 cm,
- Abnormal glow discharge between the electrodes,
- Ground shield to promote a uniform erosion rate of the target,
- Discharge current: at the cathode φ ions; at the anode: φ electrons,
- Typical operating conditions (Ni + Ar):
 - Cathode current density: 1 mA/cm²,
 - Discharge voltage: 3000 V,
 - Ar pressure: 100 mTorr,
 - Deposition rate: 40 nm/min.
- Energy of incoming particles on the substrate is low,
- Sputtered-atom transport within the negative glow is by diffusion,
- Large substrate heating effects.

3. Reactors and deposition

3.2 Magnetron system

Magnetron sputtering sources provide - relatively high deposition rates, larger deposition areas and low substrate heating

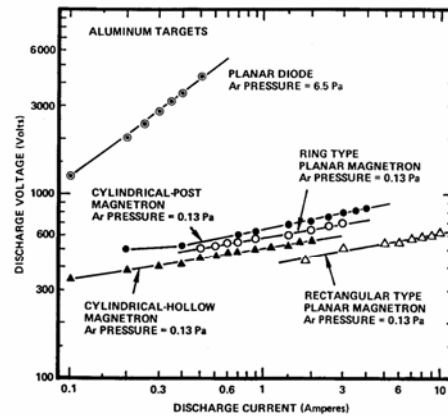


Figure 5.28. Typical current-voltage characteristics for a planar diode sputtering source and for various types of planar and cylindrical magnetrons. All sources were operated with Al targets at the Ar working-gas pressures indicated.

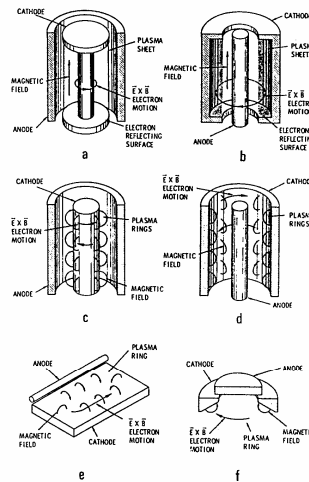
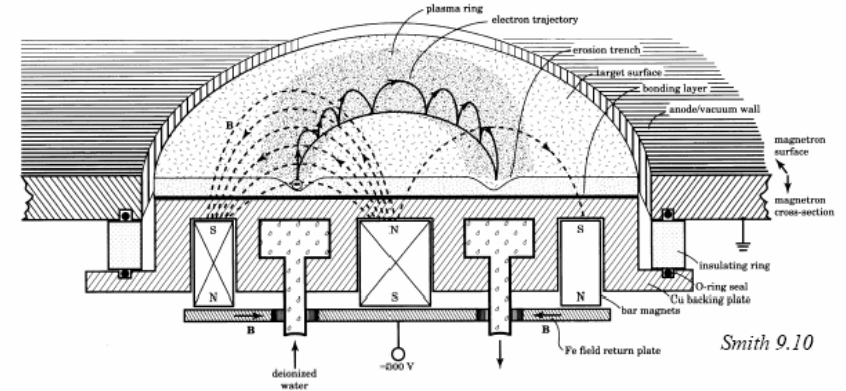


Fig. 3. The configuration of various magnetron sputtering sources: (a)-(d) are cylindrical magnetrons; (b) and (d) are often called inverted magnetrons and sometimes hollow cathodes; (a) is referred to here as a cylindrical-post magnetron and (b) as a cylindrical-hollow magnetron; (e) is the planar magnetron; (f) is often referred to as a sputter gun. In figures vector arrows are indicated by arrows over the vector quantities.

3. Reactors and deposition

3.2.1 Balanced magnetron system

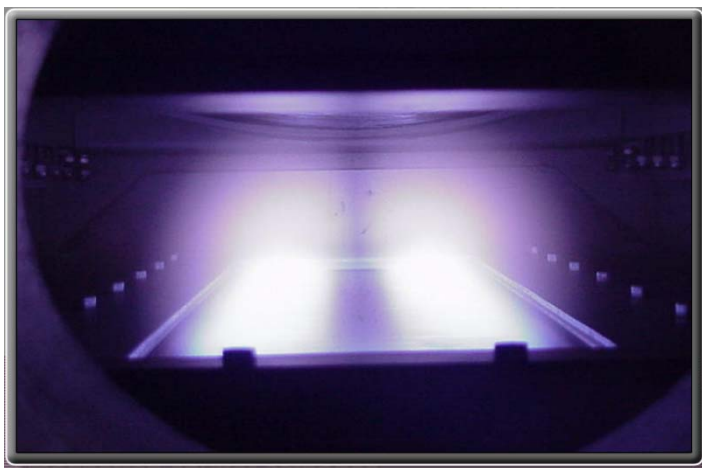
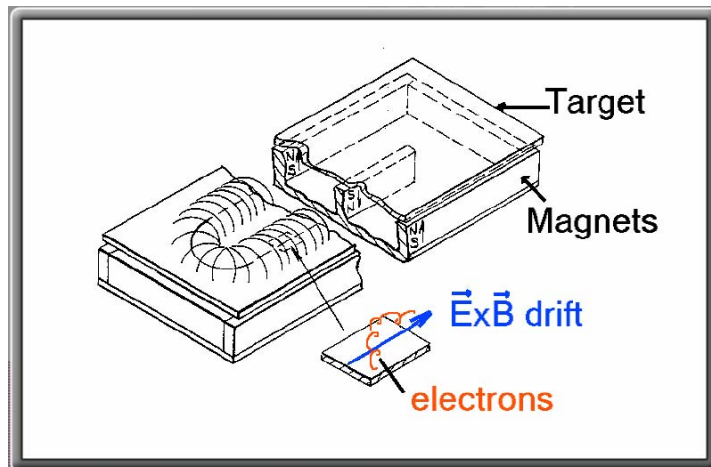


Smith 9.10

Characteristics:

- Electrode spacing: 5 -20 cm,
- Typical transverse magnetic field: 40 - 400 G.
- Typical operating conditions (cylindrical magnetrons):
 - Power density: 10-30 W/cm²,
 - Discharge voltage: 400 V,
 - Ar pressure: 1-5 mTorr,
 - Deposition rate: 1000 nm/min (Cu),
 - Erosion rate: 1 μm/min.
- Energy of incoming particles on the substrate is high,
- Small substrate heating

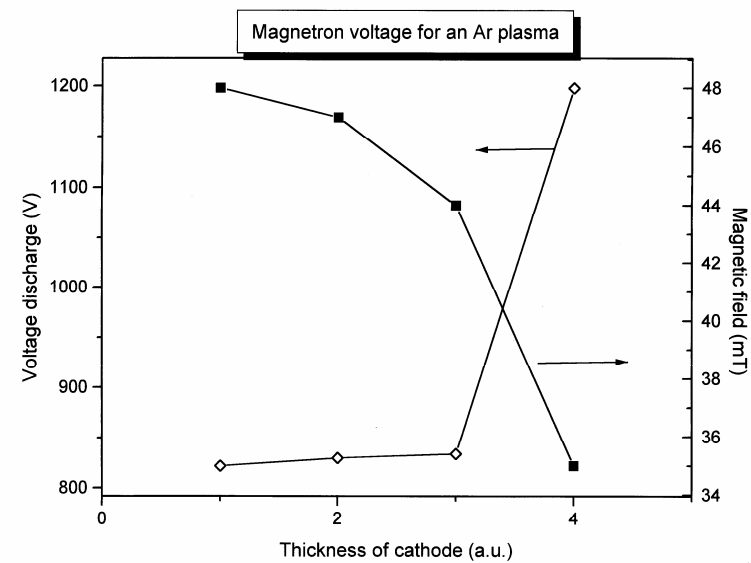
Magnetron sputtering



Novembre 2008

VII.11 Plasma, S. Lucas

3. Reactors and deposition

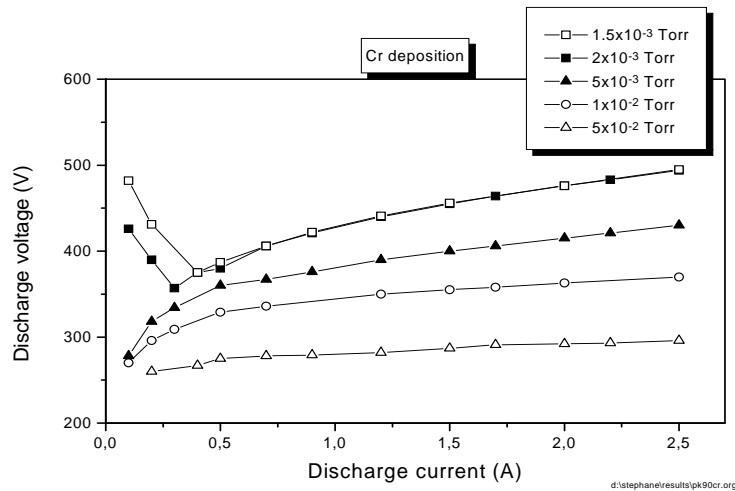


Novembre 2008

VII.12 Plasma, S. Lucas

3. Reactors and deposition

Current voltage relationship:



$$I = k.V^n$$

The more efficient is the electron trapping in the plasma, the high is n (2-6)

3. Reactors and deposition

Deposition rate:

The amount of particles sputtered from the target surface is:

$$E = \frac{j_+ S t M}{e N \rho} = 6.23 \frac{S j_+ M}{\rho} (nm/min)$$

where : j (mA/cm²), M atomic weight, ρ (gr/cm³), S sputtering yield.

The deposition rate (R) on the substrate is:

$$R = K.E$$

Where K is a constant depending on geometrical considerations (distance cathode-substrate) and scattering of target atoms by gas in the plasma (pressure): $K \approx (pD)^{-1}$

If we assume a linear relationship for S between 300 to 800 V, R is proportional to W.

The deposition rate efficiency (RE) can be defined as:

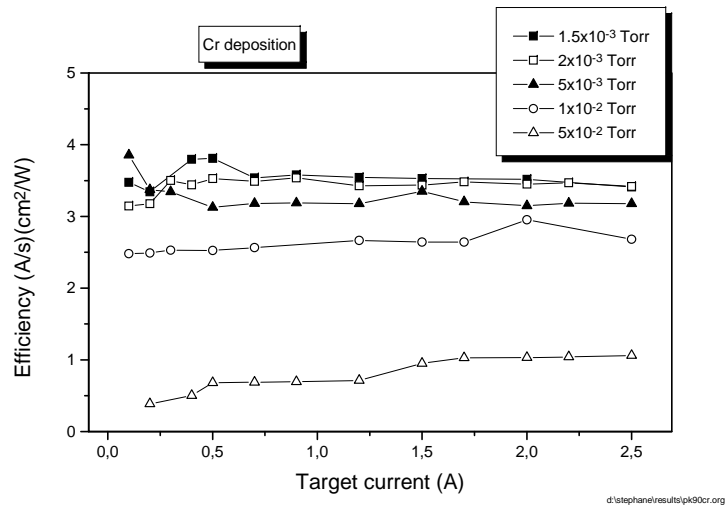
$$R_E = \frac{R (nm/min)}{P (W/cm^2)}$$

R_E is a useful concept for optimizing the deposition conditions, magnet arrangement, source-substrate spacing, ...

3. Reactors and deposition

Deposition rate efficiency:

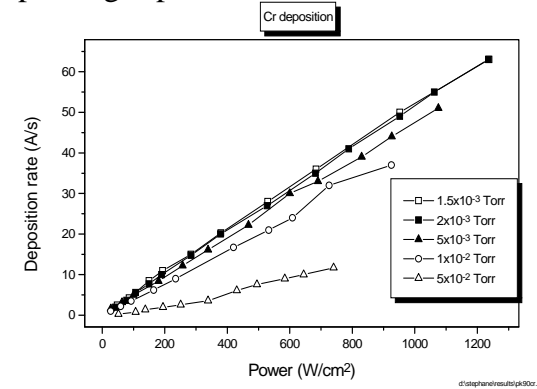
Efficiency of the DC-PM Sputtering [5]				
Cathode material	R_E (A/min)(cm ² /W)	Av. Power density (W/cm ²)	Cathode surface (cm ²)	Ar pres. (mTorr)
Cu	540	67	67	4
Cu	780	30	153	4
Cu	1020	10.5	189	4



3. Reactors and deposition

Factor limiting R:

- Max power applied to the cathode: 100 W/cm²
- Sputter gas pressure:



- Target substrate distance

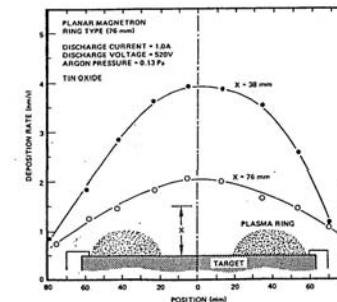


Figure 5.30. Deposition-rate profile for a ring-type planar-magnetron sputtering source at various distances from the cathode surface.

- Dielectric formation on cathode: reactive sputtering

3. Reactors and deposition

3.2.2 Unbalanced magnetron systems

Electron and ion bombardment.

- In conventional DC or RF sputtering, secondary electrons emitted by the cathode are accelerated within the dark space and will bombard the substrate with almost the full energy of the cathode potential (unless substrate is biased or shielded).
- In magnetron mode, the fast electrons are confined by the magnetic field close to the target. The thermal electrons created in the plasma are collected by the anodes.

3. Reactors and deposition

Unbalanced DC magnetron

Cathode Cu, gaz : $C_2H_2 + He$



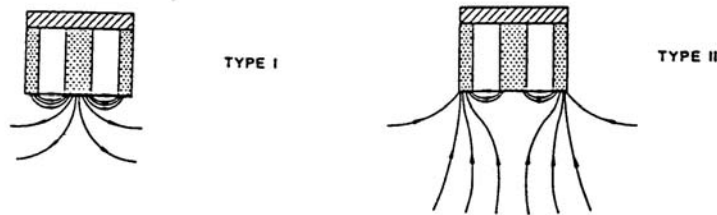
Magnétron droit

Magnétron droit +
blindage
avec plaques
épaisses

Magnétron droit sans
aimants à gauche

3. Reactors and deposition

Unbalanced DC magnetron



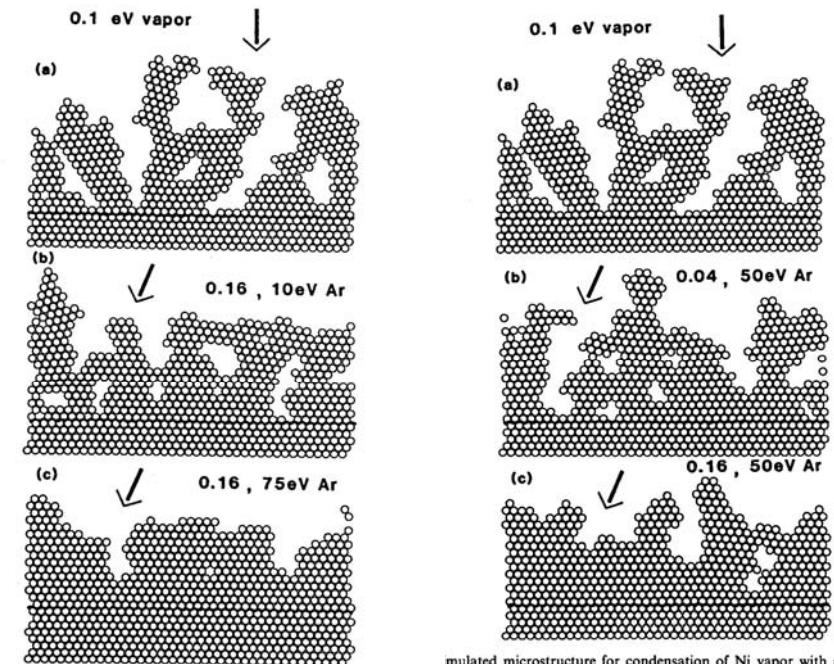
Plasma probe results for a 300 mA discharge, with a 100 mm diameter probe at 6 cm away from the cathode.

Conf.	Discharge (V)	Self bias potential (V)	Grounded probe current (mA)	-100 V probe current (mA)
I	410 → 600	+0.4 → +3	-0.5 → -2	-2 → -4
II	400 → 540	-25 → -33	264-311	-22 → -100

3. Reactors and deposition

Unbalanced DC magnetron

Effect of substrate bombardment



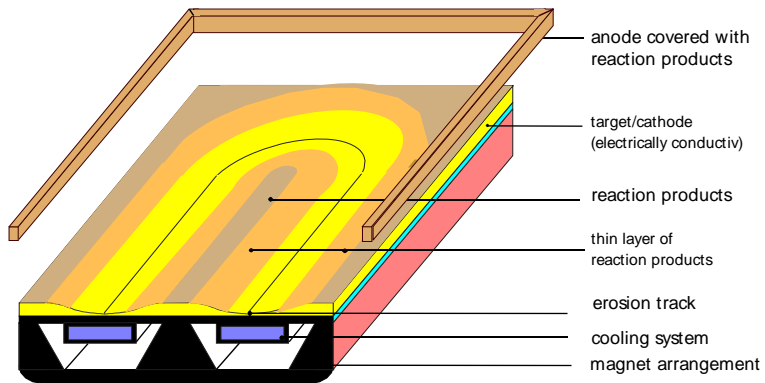
ulated microstructure for condensation of Ni vapor with a k normal to the substrate surface (a) in the absence of ion bombardment (b) with a flux ratio $J_i/J_v = 0.16$, and (c) with a flux ratio $J_i/J_v = 0.16$. After Müller (8).

ulated microstructure for condensation of Ni vapor with a k normal to the substrate surface (a) in the absence of ion bombardment (b) with a flux ratio $J_i/J_v = 0.04$, and (c) with a flux ratio $J_i/J_v = 0.16$. After Müller (8).

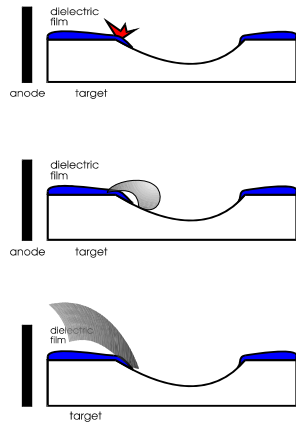
3. Reactors and deposition

3.2.3 Reactive sputtering

Ex: Al target + Ar + O₂



basic mechanism

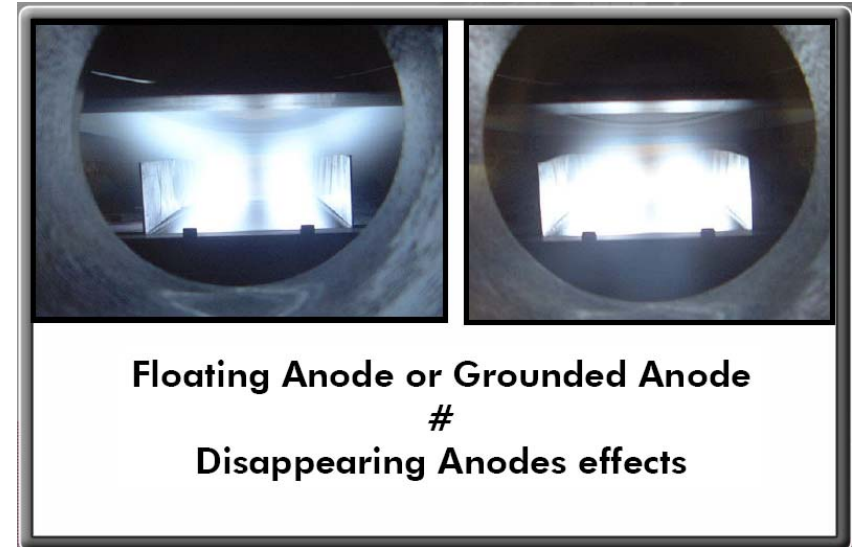


Novembre 2008

VII.21 Plasma, S. Lucas

© 2004 L'Oréal

3. Reactors and deposition



Novembre 2008

VII.22 Plasma, S. Lucas

3. Reactors and deposition

Ar + gaz réactif

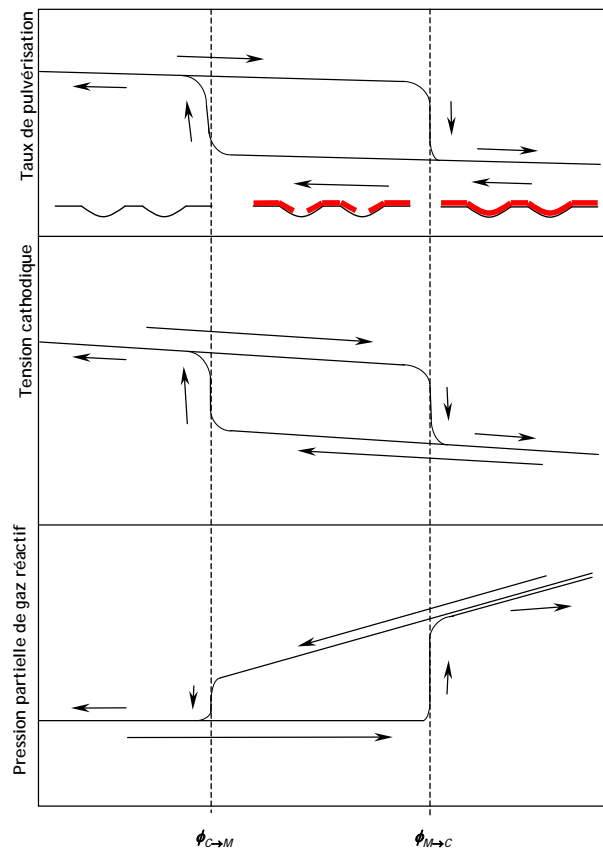


Figure 1 - 20 : illustration des variations de la pression partielle, de la tension cathodique et du taux de pulvérisation en fonction du flux de gaz réactif introduit au sein d'une décharge cathodique [Hf98].

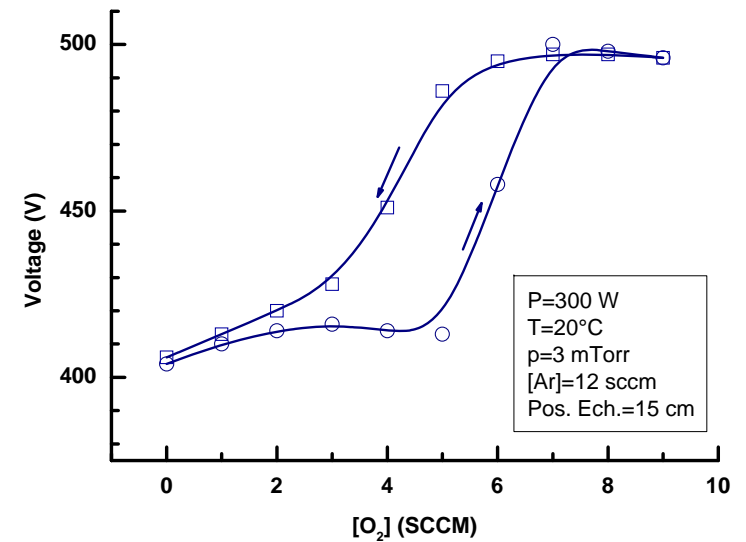
Novembre 2008

VII.23 Plasma, S. Lucas

3. Reactors and deposition

Reactive deposition: TiO₂ case

Ti/TiO₂ hysteresis curve



Novembre 2008

VII.24 Plasma, S. Lucas

3. Reactors and deposition

Reactive deposition: TiO₂ case

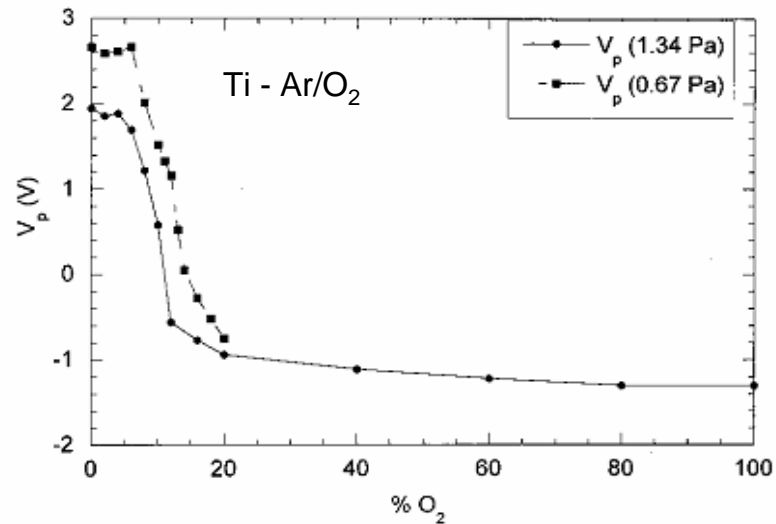


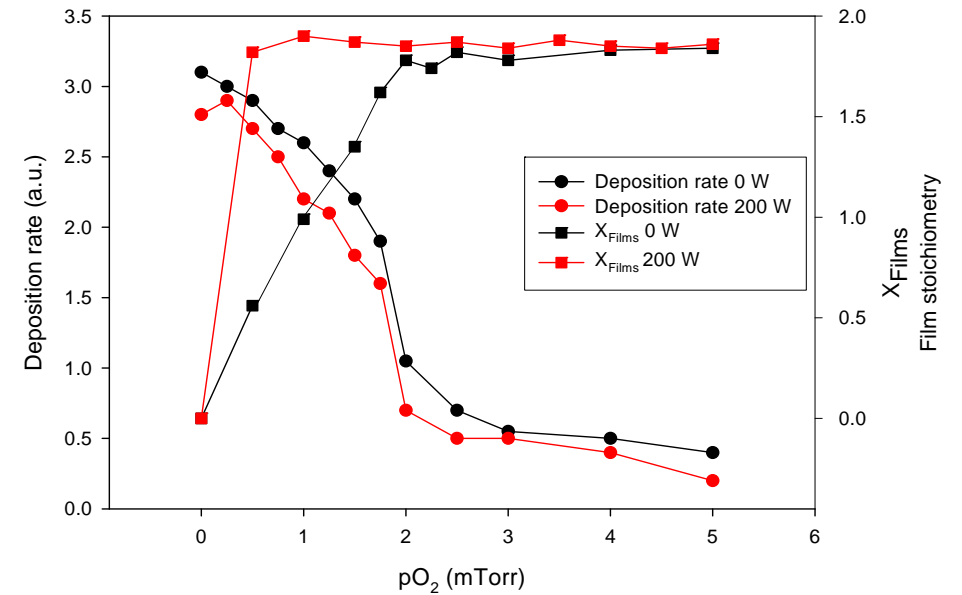
FIG. 4. Plasma potential as a function of the gas composition at two pressures and with $I_d=495$ mA.

Vancoppenolle et al, J. Vac. Sci. Technol. A 17-6,1999, 3317.

3. Reactors and deposition

Reactive deposition: SnO₂ case (from R. Snyder, UMH)

Consider just the black points



R. Snyders et al., Plasm. Proc. Polym., 2007

3. Reactors and deposition

Berg's Model (JVST, A 5(2) 1987)(SCT, 49(1991)336):

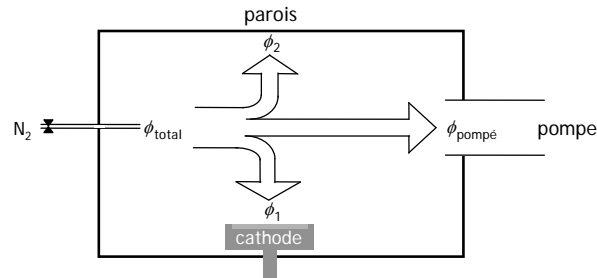


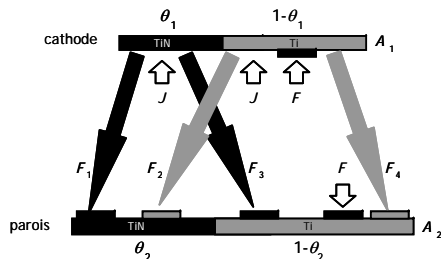
Figure 1 - 23 : Schéma illustrant les flux de gaz réactif entrant et sortants.

surface où il n'existe pas de réaction est donnée par $(1 - \theta)$. Pour simplifier le problème, il semble judicieux d'émettre l'hypothèse non vérifiée [PL84, Ro95] mais utile que le TIN pulvérisé se dépose sans se dissocier. Comme l'illustre la figure 1-24, il suffit alors de six flux pour décrire le phénomène de pulvérisation:

- F_1 : TIN pulvérisé depuis la partie nitrurée de A_1 vers la partie déjà nitrurée de A_2 .
- F_2 : TI pulvérisé depuis la partie non nitrurée de A_1 vers la partie déjà nitrurée de A_2 .
- F_3 : TIN pulvérisé depuis la partie nitrurée de A_1 vers la partie non nitrurée de A_2 .
- F_4 : TI pulvérisé depuis la partie non nitrurée de A_1 vers la partie non nitrurée de A_2 .
- F : N_2 libre dû à la pression partielle et uniquement consommé par les parties non nitrurées:

$$F = \frac{p_N}{\sqrt{2\pi \cdot kT}} \quad (\text{Eq. 1 - 42})$$

- J/e : Flux Ar^+ décapant la cathode.

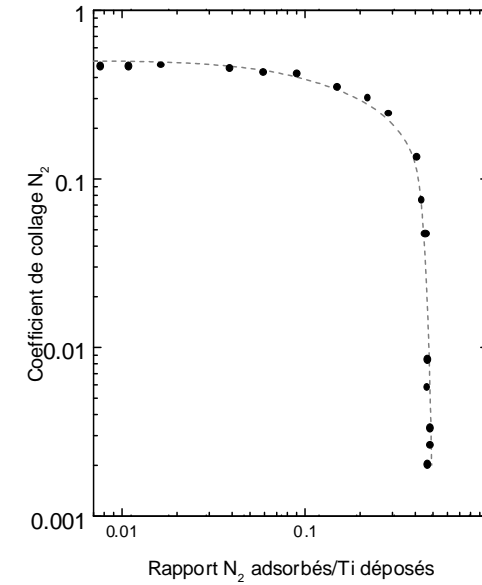


$$\begin{aligned} \phi_1 &= \alpha_1 F (1 - \theta_1) A_1 \\ \phi_2 &= \alpha_2 F (1 - \theta_2) A_2 \\ \phi_{pompe} &= p_N \cdot V_{pompe} \end{aligned}$$

$$\begin{aligned} \phi_{tot} &= \alpha_1 F (1 - \theta_1) A_1 + \\ &\quad \alpha_2 F (1 - \theta_2) A_2 \\ &\quad + p_N \cdot V_{pompe} \end{aligned}$$

sma, S. Lucas

3. Reactors and deposition



Novembre 2008

VII.28 Plasma, S. Lucas

3. Reactors and deposition

$$R = [S_{TiN} \cdot \theta_i - S_{Ti} \cdot (1 - \theta_i)] \cdot \frac{J}{e} \quad (\text{Eq. 1 - 48})$$

Seulement huit paramètres sont utilisés pour construire des graphes $p_N = f(\phi_{tot})$ et $R = f(\phi_{tot})$: les coefficients de pulvérisation du Ti et TiN, les coefficients de collage, le courant, la vitesse de pompage, et enfin, les surfaces de la cathode et de dépôt. Ces trois derniers paramètres sont les seuls qui dépendent de l'installation utilisée pour le dépôt.

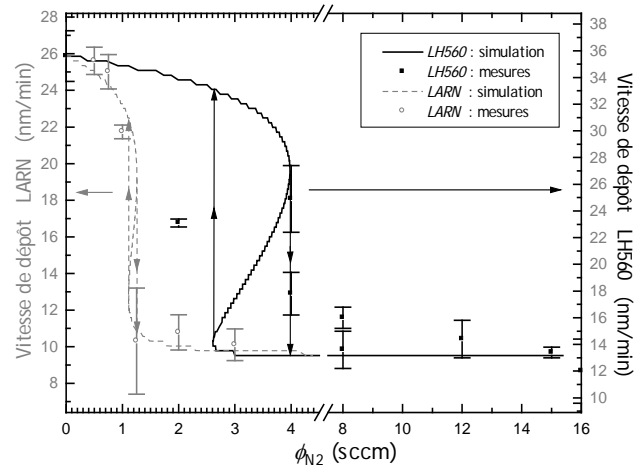


Figure 3 - 16 : présentation des résultats du modèle de *Berg* où est ajouté la mesure de l'évolution de la vitesse de dépôt du nitrure de titane (cercles) en fonction du flux de gaz réactif avec la pression et la puissance au sein de la décharge cathodique constante ($p = 0.27$ Pa et $P = 11.7$ W/cm²) dans l'enceinte de *LARN* ($d = 150$ mm) avec une géométrie ouverte et dans l'installation *LH560* (carrés).

Novembre 2008

VII.29 Plasma, S. Lucas

3. Reactors and deposition

TiN

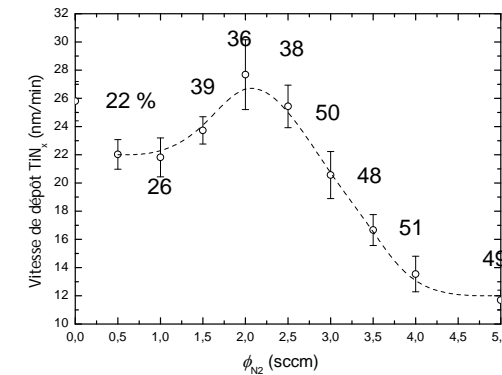


Figure 3 - 17 : évolution de la vitesse de dépôt du nitrure de titane en fonction du flux de gaz réactif à pression totale et puissance relative maintenues constantes au sein de la décharge cathodique ($p = 0.27$ Pa & $P = 11.7$ W/cm²) dans l'enceinte du *LARN* ($d = 150$ mm) avec une géométrie fermée et une injection Ar et N₂ différenciée (la courbe ne sert qu'à guider l'œil).

Novembre 2008

VII.30 Plasma, S. Lucas

3. Reactors and deposition

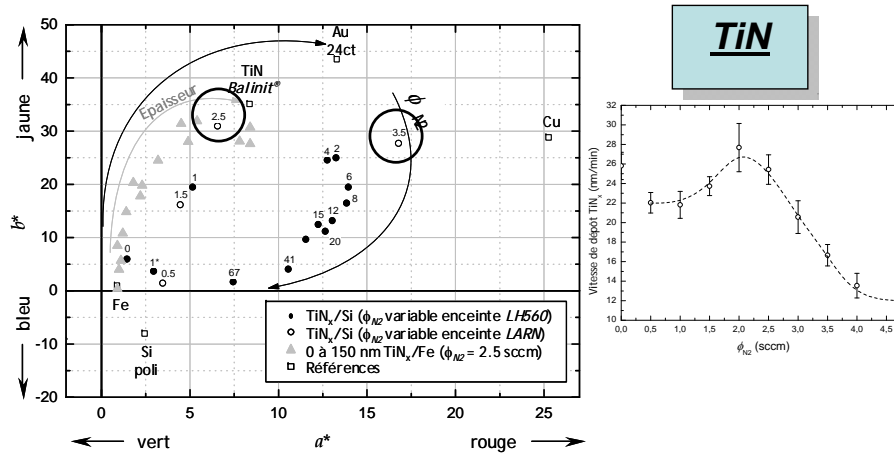


Figure 4 - 13 : mesures colorimétriques présentées dans le plan a^*, b^* pour différentes couches TiN_x (≥ 200 nm, 11.7 W/cm 2 , 0.27 Pa) recouvrant du Si monocristallin poli et réalisées sous différents flux N_2 comme indiqué en regard des points de mesure dans les deux enceintes de dépôts (cercles pleins dans *LH560* et cercles ouverts au *LARM*). Les carrés représentent quelques données de référence tandis que les triangles gris reprennent les données obtenues en fonction de l'épaisseur de la couche TiN_x déposée.

Pour les couches TiN_x déposées sur substrats de silicium monocristallin poli, une évolution de la couleur du gris au jaune doré en terminant par le bronze a été observée si la quantité d'azote dans le plasma augmente. Cette progression a également été relevée par nombre d'auteurs [Th86,Pe88,St90,Je92,Re92,No99]. La région de transition où apparaît la couleur jaune-or caractérise également le changement de régime de pulvérisation, la décharge part du mode métallique (gris à gris jaune) pour arriver au mode nitrure (jaune puis bronze et brun). Il existe en effet une corrélation entre les pourcentages N_2 caractérisant cette transition vers le jaune doré et ceux relevés lors de l'étude des vitesses de dépôt autour de 2 et 4 sccm N_2 . Cette observation se retrouve également dans la littérature.

Novem

3. Reactors and deposition

TiN

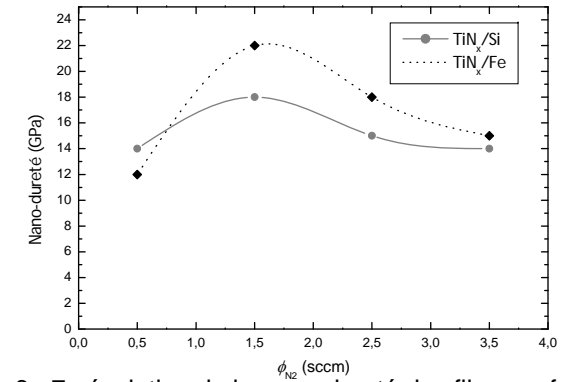
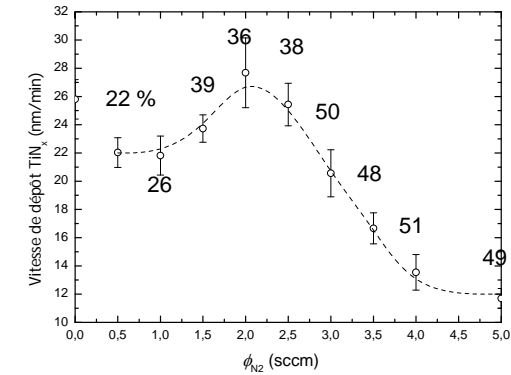


Figure 6 - 7 : évolution de la nano-dureté des films en fonction du ϕ_{N_2} pour du TiN_x (500 nm, 0.27 Pa, 11.7 W/cm 2) déposé sur substrat de silicium poli et de *fer noir* non poli.



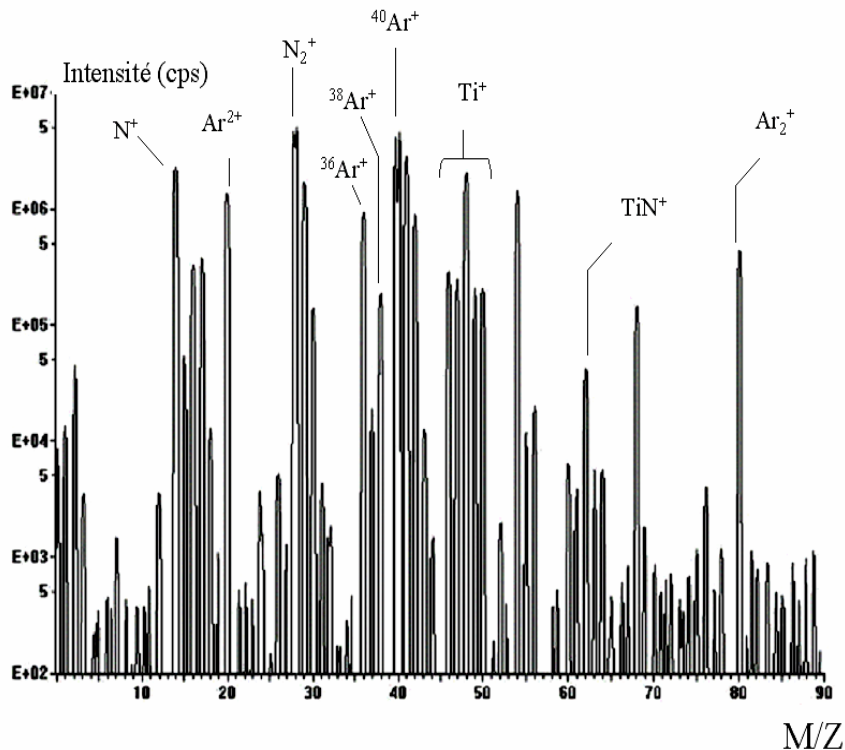
Novembre 2008

VII.32 Plasma, S. Lucas

3. Reactors and deposition

TiN: mass spectrum (From S. Konstandinis, UMH)

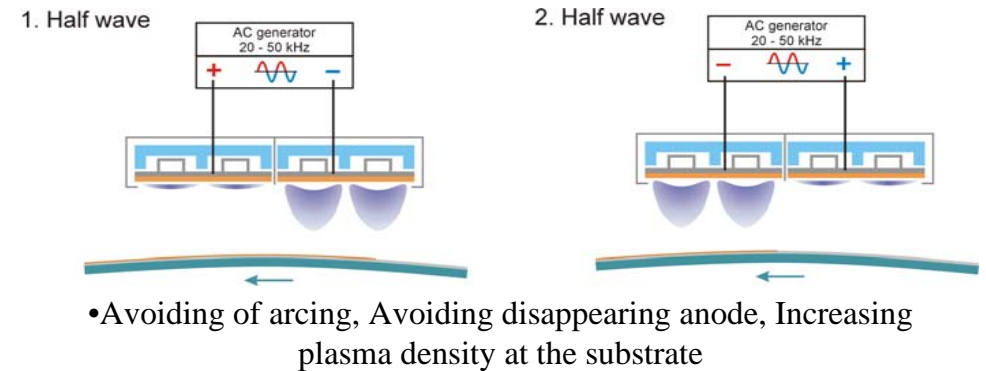
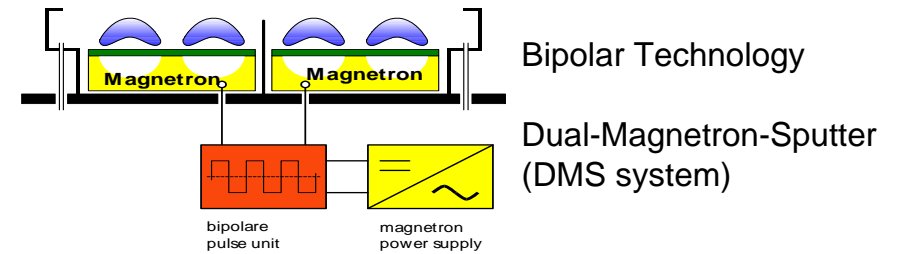
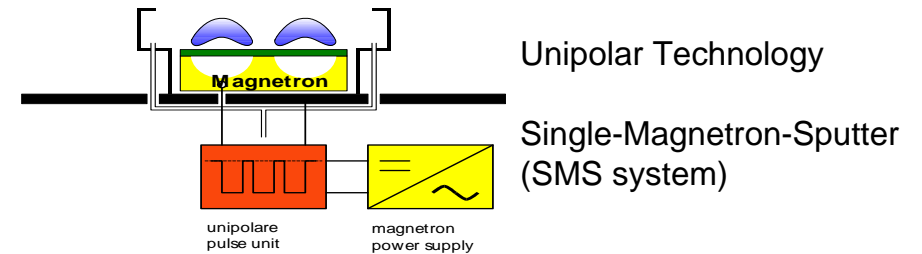
- Rapport m/z : N_2^+ et CO^+ ont le même m/z !
- Ions « exotiques » car chimie en phase gazeuse *hors équilibre* :
 - ArH^+ (m/z = 41), Ar_2^+ (m/z = 80), TiN^+ (m/z = 62)...
- Répartition isotopique aide à l'identification :
 - Ti^+ à m/z = 46, 47, 48, 49, 50. Valable aussi pour TiN^+ .
 - Ar^+ à m/z = 36, 38 et 40



3. Reactors and deposition

3.2.4 Pulsed magnetron

Avoid arcing and increase substrate bombardment



Novembre 2008

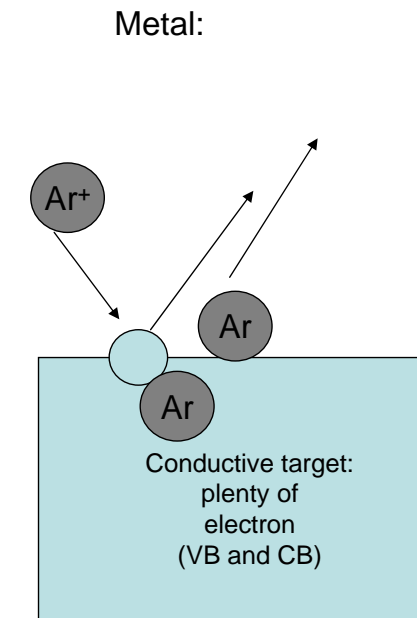
VII.34 Plasma, S. Lucas

3. Reactors and deposition

- Multiple mechanism promote the formation of arc:
 - Localized charging at the surface of the target (inclusions or impurities, insulating area, ...)
 - Charge accumulation (Ion bombardment)
 - Electric field exceeds dielectric strength
 - Discharge toward the closest conductive point

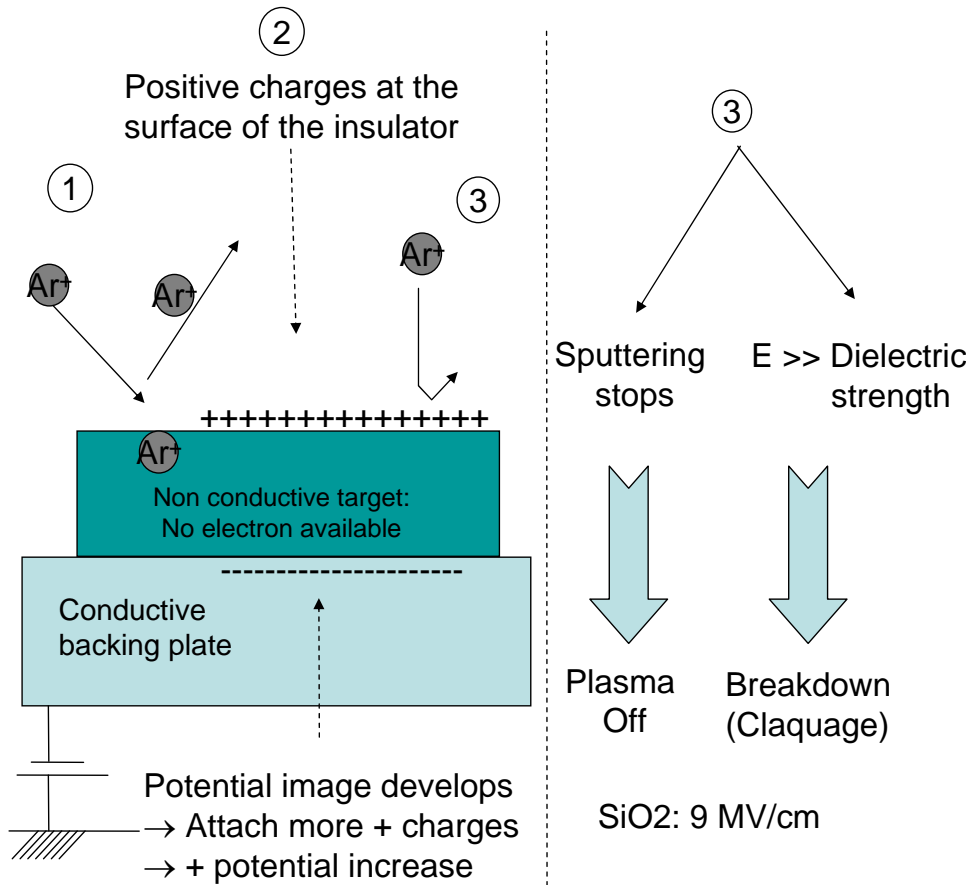
3. Reactors and deposition

- Insulators can be sputtered for a short time by DC PSU.



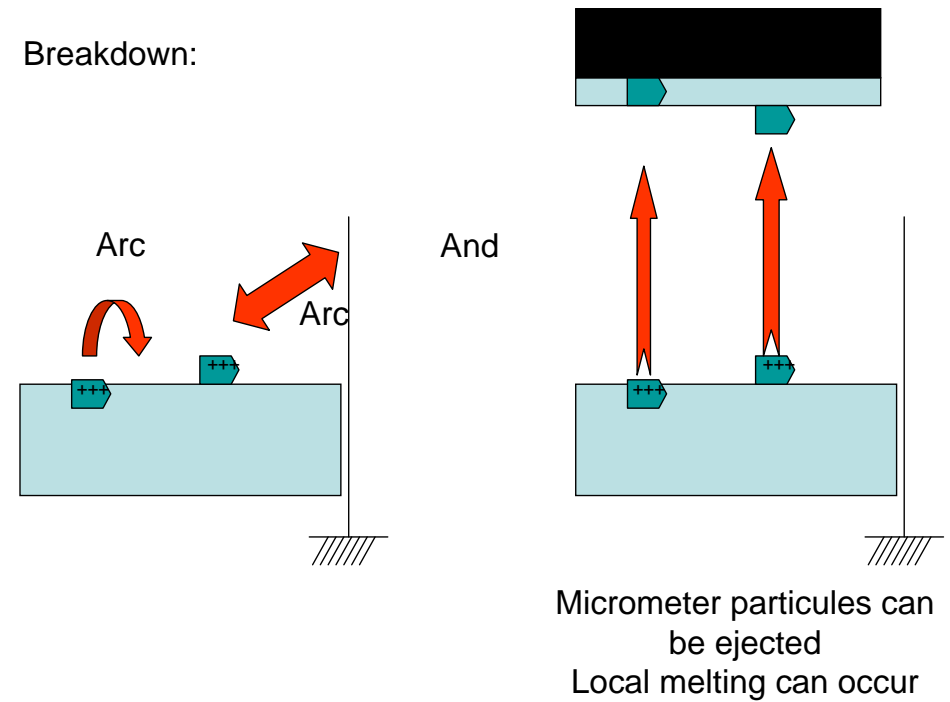
3. Reactors and deposition

DC sputtering of insulator



3. Reactors and deposition

Breakdown:

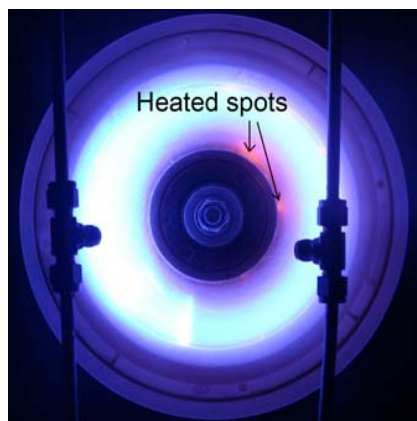
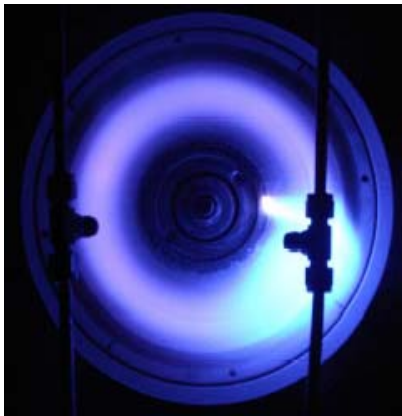


Unneeded particulates in the films and potential holes in the films

3. Reactors and deposition

Causes of arcs

- Small local disruption at the cathode surface:
 - Inclusions as gas pockets, voids, grain boundaries, oxides, ...
 - Magnetic dirt attracted by magnetic field
 - Adsorbed contaminants (Water, ...) coming out of the target causing local pressure variations,
 - Local Surface Temperature variations -> thermal electrons (Poor bond, cooling channel blocked, ...)

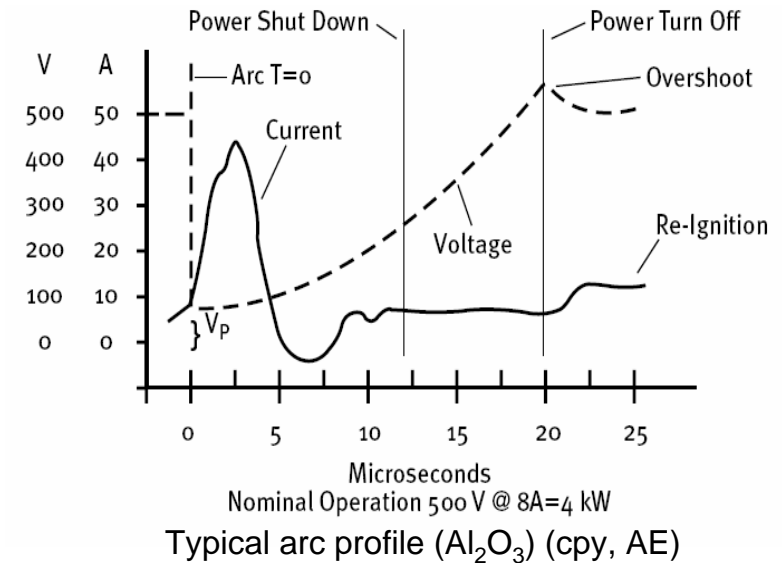


Novembre 2008

VII.39 Plasma, S. Lucas

3. Reactors and deposition

Arc management by the PSU



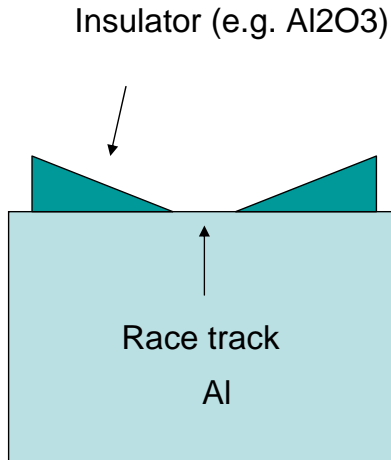
- Materials with relatively high melting point, such as Ti, Ta, and Cr have a very low tendency to arc, while materials with relatively low melting point, like Cu and Al, have a higher tendency to arc.

Novembre 2008

VII.40 Plasma, S. Lucas

3. Reactors and deposition

Why pulsed plasma ?



$$C = \frac{\epsilon_0 \epsilon_T A}{d}$$

and

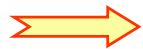
$$Q = C.V = J.A.T$$

$$E = \frac{V}{d}$$

$$\text{Time for breakdown} = \frac{\epsilon_t \cdot \epsilon_0 \cdot E_b}{J}$$

It does not depend on thickness of the insulator

For Al_2O_3 : $\epsilon_t = 10$, $E_b = 10^8 \text{ V/m}$

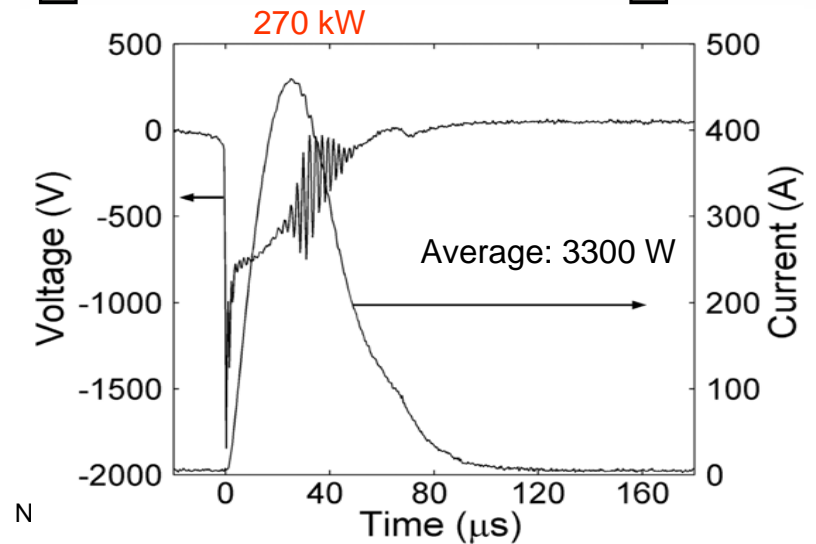
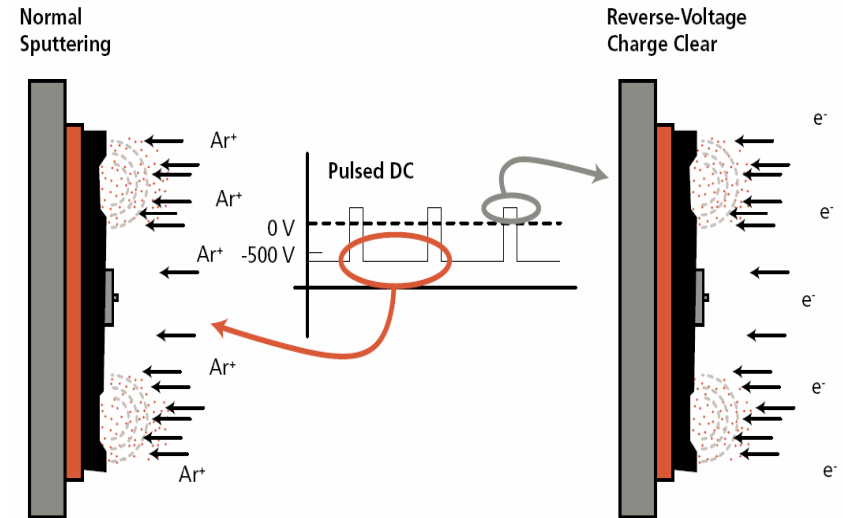


$T = 50 \mu\text{S}$ for 100 mA/cm^2

If pulsed at 20 kHz, arc formation is prevented

3. Reactors and deposition

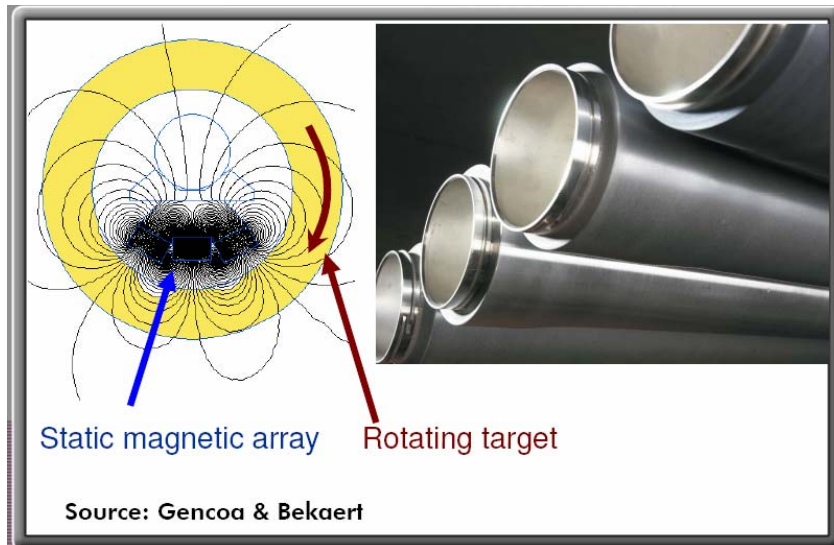
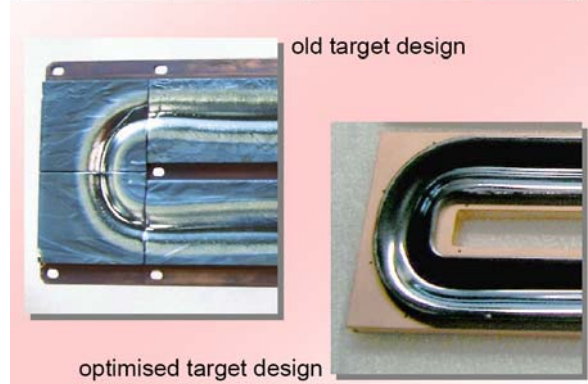
Pulsed PSU



3. Reactors and deposition

3.2.5 Special magnetron

Actual Developments to Improve Reactive Sputtering



Novembre 2008

VII.43 Plasma, S. Lucas

3. Reactors and deposition

3.3 RF Reactors

The operating frequency is usually 13.56 MHz, or higher harmonics. (Allotted by the International Communication Authorities).

The generators are designed to operate at constant output impedance 50Ω . Since the impedance of glow discharge depends on plasma parameters, a matching unit is necessary to reduce as much as possible the reflected power.

3.3.1 Electrodeless discharges

Power is coupled to the plasma across a dielectric window or all. Since no powered electrodes are present within the plasma, there is only low voltage (20 → 40 V) across all plasma sheaths at electrodes or wall surfaces.

Novembre 2008

VII.44 Plasma, S. Lucas

3. Reactors and deposition

RF Reactors

Electrodeless discharges

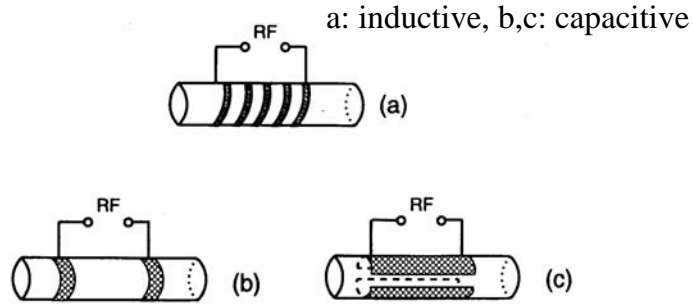
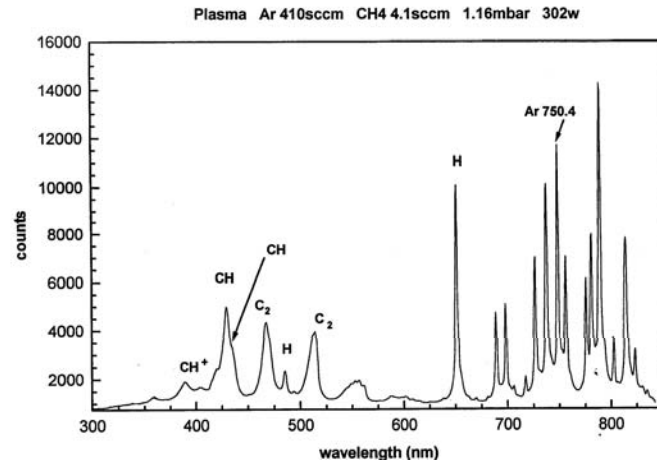


Fig. 4-3 RF coupling methods to electrodeless reactors.

Inductive, CH₄ & Ar plasma

é are accelerated by the induced electric field inside the coil



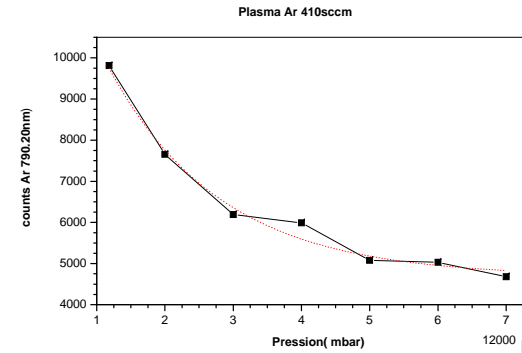
Novembre 2008

VII.45 Plasma, S. Lucas

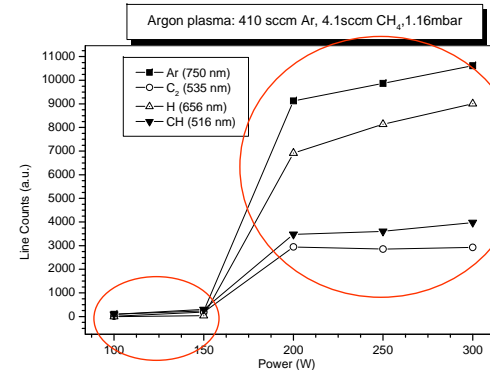
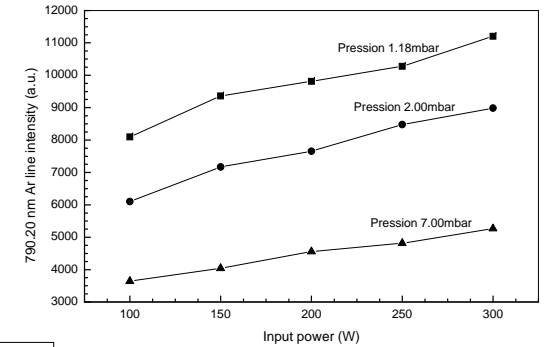
3. Reactors and deposition

RF Reactors

Inductive, CH₄ & Ar plasma



Ar plasma in an inductive RF reactor



Low power: capacitive coupling
High power: inductive coupling

à, S. Lucas

3. Reactors and deposition

RF Reactors

Inductive

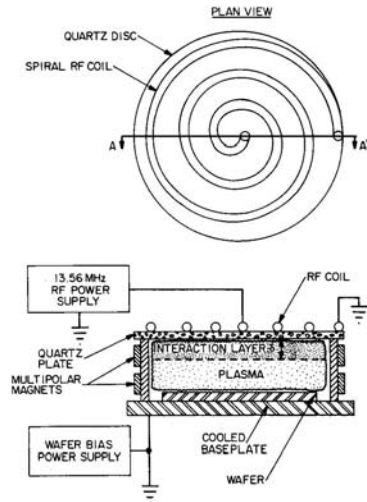


Figure 11.16 Schematic of an inductive parallel plate reactor. Top: plan view showing flat spiral RF coil on top surface of the reactor. Bottom: elevation through section AA' showing cross-section of inductive parallel plate reactor.

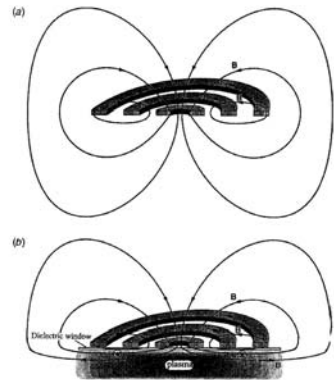
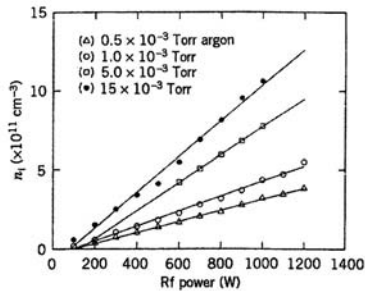


Figure 12.7. Schematic of the rf magnetic field lines near a planar inductive coil (a) nearby plasma and (b) with nearby plasma (after Wendt, 1993).



10. Ion density versus rf power and argon pressure (Hopwood et al., 1993b).

Hopwood, 1993

Gogyak, 1994

7 Plasma, S. Lucas

3. Reactors and deposition

3.3.2. RF Reactors with electrodes

Diode

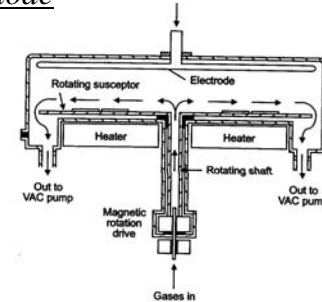


Fig. 4-7 Diagram of a radial flow reactor (from [12], reprinted with permission from Thin Solid Films, vol. 113, p. 135, 1984).

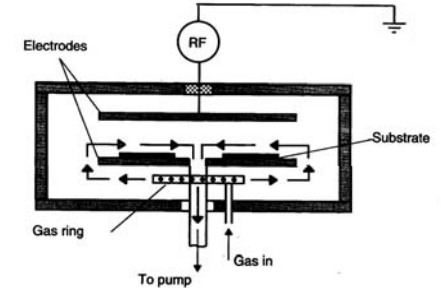


Fig. 4-6 Diagram of a Reinberg reactor.

- Discharge mainly confined between the electrodes.
- Possible plasma contamination with atoms sputtered from electrodes
- Careful gas distribution must be achieved.
- Impossible to dissociate ion energy and flux.

Triode

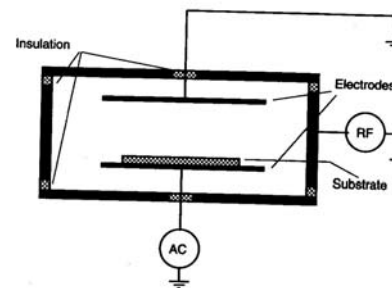


Fig. 4-8 Power coupling to a planar triode reactor.

When both electrodes are insulated from the walls. Each electrode and the reactor wall can be powered independently, and each be biased, floating or grounded. \Rightarrow control of ion energy and flux.

Novembre 2008

VII.48 Plasma, S. Lucas

3. Reactors and deposition

3.4 Microwave reactors

3.4.1 Non ECR microwave reactors

Microwave must be transmitted through wave guides, whose cross section is determined by the wavelength of the microwave ($2.45 \text{ GHz} = 7.21 \text{ cm}$).

- 1: A microwave PSU of constant frequency but variable power
- 2: A circulator to protect the PSU from large reflected power due to unmatched μW applicator
- 3: Meters to monitor both incident and reflected power
- 4: An impedance matching unit

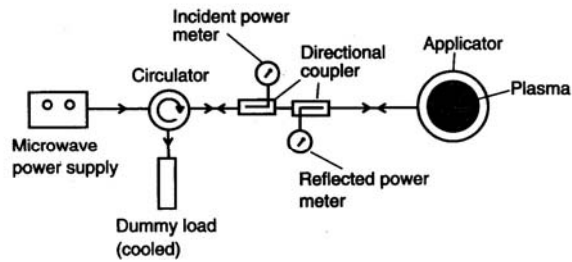


Fig. 4-11 Diagram of microwave power system for cold plasma excitation.

μW applicator:

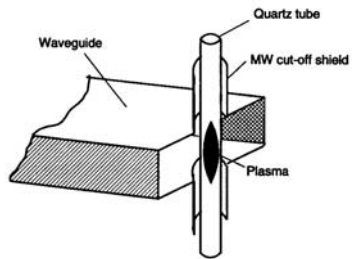


Fig. 4-12 Waveguide-tube μW applicator. An axisymmetric microwave coupler (from [18], reprinted with permission from *Research & Development Magazine*, October, 1989, by Cahners Publishing Company).

3. Reactors and deposition

3.4.2 ECR Microwave reactors

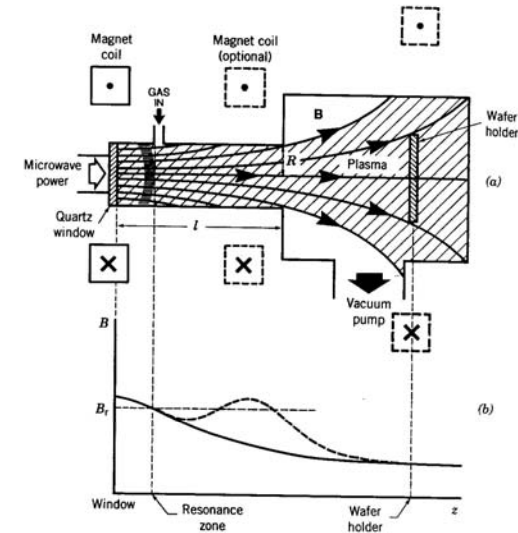


FIGURE 13.1. A typical high-profile ECR system: (a) geometric configuration; (b) magnetic field variation, showing one or more resonance zones. (From "Design and Density Sources for Materials Processing" from the work "Physics of Thin Films," Vol. 1, Academic Press, Inc., Publisher in Press)

- Since electrons diffuse faster than ions into the processing chamber, they create an electric field which causes the extraction of ions.
- Sometimes, additional magnetic field is added close to the sample to achieve better control of ion direction and confine the plasma.

3. Reactors and deposition

When additional ion energy control is needed:

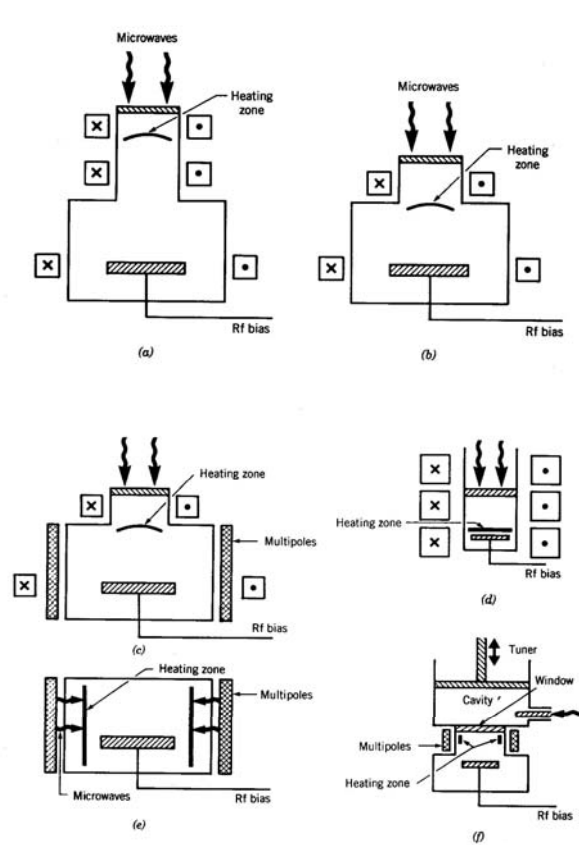


FIGURE 13.4. Common ECR configurations: (a) high aspect ratio; (b) low aspect ratio; (c) low aspect ratio with multipoles; (d) close-coupled; (e) distributed (DECR); (f) microwave cavity excited. (From "Design of High-Density Sources for Materials Processing" from the work "Physics of Thin Films," Vol.18, by Academic Press, Inc., Publisher in Press)